ANTIOXIDANTS & REDOX SIGNALING
Volume 00, Number 00, 2019

DOI: 10.1089/ars.2019.7878

Hemeproteins as Targets for Sulfide Species

Fernando Martín Boubeta,[1] Silvina Andrea Bieza,[1] Mauro Bringas,[1,2] Juan Cruz Palermo,[1] Leonardo Boechi,[3] Darío Ariel Estrin,[1,2] and Sara Elizabeth Bari[1]

Abstract

Significance: Sulfides are endogenous and ubiquitous signaling species that share the hemeproteins as biochemical targets with O_2, nitric oxide, and carbon monoxide. The description of the binding mechanisms is mandatory to anticipate the biochemical relevance of the interaction.
Recent Advances: The binding of sulfide to ferric hemeproteins has been described in more than 40 systems, including native proteins, mutants, and model systems. Mechanisms of sulfide binding to ferric hemeproteins have been examined by a combination of kinetic and computational experiments. The distal control of the association process, dissected into the migration of the ligand to the active site and the binding event, reveals that neutral hydrogen sulfide (H_2S) reaches the active site and is the predominant binding ligand, while the HS^- is excluded by the protein matrix. Experiments with model compounds, devoid of a protein scaffold, reveal that both H_2S and HS^- can bind the ferric heme if accessing the site. A critical role of the proximal ligand in the prevention of the metal-centered reduction has been experimentally assessed. For metmyoglobin and methemoglobin, the coordination of sulfide leads to noncanonical functions: sulfide storage and its oxidative detoxification have been evidenced under physiological and excess sulfide concentrations, respectively.
Critical Issues: The bound species is suggested to predominate in the monoprotonated form, although spectroscopic evidence is pending.
Future Directions: A description of the role of hemeproteins as biochemical targets for inorganic sulfide requires understanding the reactivity of bound sulfide, for example: the metal-centered reduction, the reaction with excess sulfide, oxidants, or other gasotransmitters, among other biomolecules. *Antioxid. Redox Signal*. 00, 000–000.

Keywords: hemeproteins, sulfide, reactive sulfur species, sulfide migration, sulfide binding

Introduction

Hydrogen sulfide (H_2S) is a colorless gas with toxicity comparable with that of hydrogen cyanide that is present in animals, plants, and microorganisms in nontoxic concentrations with diverse physiological roles (1). Along with nitric oxide (NO) and carbon monoxide (CO), H_2S is a member of a group of intracellular signaling molecules called gasotransmitters, gathered for their gaseous, endogenous, and toxic nature beyond the physiological concentrations, but with a regulatory role derived from the interaction with shared biochemical targets, or by the chemical cross talk among them or other related species (45, 64). H_2S is biosynthesized from L-cysteine after the action of a cystathionine-β synthase, cystathionine γ lyase, and a 3-mercaptopyruvil sulfuryl transferase (3-MST) (27, 30). Until 1996, when the role of H_2S as a neuromodulator was revealed, the endogenous production of H_2S was only considered a metabolic waste.

The physiological concentration of H_2S in mammalian tissues is a subject of active debate, but is generally accepted to be in the low micromolar region (31, 60). Both the excess and the deficiency of H_2S have been related to pathologic

[1]Instituto de Química Física de los Materiales, Medio Ambiente y Energía. (INQUIMAE) CONICET, Universidad de Buenos Aires, Buenos Aires, Argentina.
[2]Departamento de Química Inorgánica, Analítica y Química Física, Facultad de Ciencias Exactas y Naturales, Universidad de Buenos Aires, Buenos Aires, Argentina.
[3]Facultad de Ciencias Exactas y Naturales, Instituto de Cálculo, Universidad de Buenos Aires, Buenos Aires, Argentina.

events (35, 60). Low-molecular-weight thiols, protein thiols, and metalloproteins—with the ferric center of hemeproteins as constituents of proteins, enzymes, transcription factors, membrane ion channels (55) —have been recognized as biochemical targets for inorganic sulfide (42), and their interactions should be considered in the molecular description of potential therapeutic objectives for sulfide (55). While the participation of the interaction of sulfide species and thiol compounds in biologically relevant processes has been and is still being extensively studied (persulfidation or S-sulfhydration processes) (22), the chemistry and mechanisms of sulfide binding to hemeproteins forming coordination complexes have been less appraised. The subject has actively grown in the last decade to provide tools for the inspection of the outcomes of the interaction, and eventually to focus on the use of hemeproteins as pharmacological targets for sulfide donors.

Among heme-containing proteins, the reactivity of sulfide toward their ferric forms is remarkable because it is known to rule the inhibition of the cytochrome c oxidase, by binding and reducing the ferric heme iron and coordinating with the ferrous form assisted by the copper center, thus hampering O_2 respiration (16, 47). Less dramatic, but very interesting from a structural and functional standpoint, is the binding of sulfide to the ferric form of hemoglobin I from *Lucina pectinata*, a clam inhabiting sulfide-rich environments, with a very high-affinity constant (33, 34). This case was the first evidence of sulfide binding to a methemoglobin, and significantly triggered the interest in the coordination chemistry of sulfide to hemeproteins.

The attempts to understand the different chemical behaviors require the dissected analyses of the role of neighboring amino acids or other functional structures, defining a distal and proximal site (12), for the formation and stabilization of the coordination complex. The distal mechanisms encompass the possibilities of migration of the potential ligand from the bulk to the active site, and the final binding to the ferric heme. As the state-of-the-art covers mostly the interaction of sulfide with hemoglobins, the proximal mechanisms for the stabilization of ligands to heme compounds encompass the interactions of the hydrogen on the Nδ of the conserved histidyl residue acting as fifth ligand, with acceptor surrounding amino acids.

To describe the reaction mechanisms where sulfides participate, it is also necessary to take into consideration the intrinsic complexity of the ligand. From the acid-base perspective, the term inorganic sulfide encompasses the neutral H_2S, and the two anionic conjugated bases hydrosulfide and sulfide, HS^- and S^{2-}, with $pK_{a1} = 6.98$ and 6.76, at 25°C and 37°C,[22] respectively, and an accepted value of $pK_{a2} = 19 \pm 2$, with reported values covering a range of eight orders of magnitude (28, 59). This acid-base behavior is a distinctive feature of H_2S among gasotransmitters, as NO and CO lack this chemical reactivity. This anticipates lipid or water solubility favoring the neutral H_2S or the anionic HS^- species, respectively. Significantly, the solubility of H_2S in water, explained in terms of a weak hydrophobic solvation, promoted studies of the partition coefficient of H_2S in water and liposome membranes, to address the potential biological distribution of sulfide species (19, 56).

The reactive sulfide species scenario is still more complicated, as it has been recently reported that the 3-MST can also form hydropolysulfides, H_2S_n ($n > 1$), and that some of the roles attributed to H_2S are a consequence of the action of H_2S_n and not of H_2S (31). The reaction between H_2S and NO is also capable of forming H_2S_n, along with nitroxyl (HNO/NO^-) and nitroso persulfide ($SSNO^-$) (5, 23, 24). These cross talk derived species are also part of the complex network capable of mediating roles for H_2S (and NO) from hemeprotein platforms (17, 18). Regarding the redox potential, as sulfide species are in the lowest oxidation state that sulfur can achieve, they are reducing agents, and the reduction potential for the two-electron process at pH 7 is $E^{\circ\prime}$ (S°/HS^-) = –0.27 V, comparable with the formation of the biologically relevant glutathione disulfide and cystine [$E^{\circ\prime}$ (GSSG/GSH) = –0.24 V at 40°C, and $E^{\circ\prime}$ (CysSSCys/CysSH) = –0.34 V] (37). At neutral pH, the one-electron reduction potential is $E^{\circ\prime}$ ($S^{\bullet-}$, H+/HS^-) = 0.91 V, and as the first pK_a of H_2S is approximately (*ca.*) 7, it can be derived that the $E^{\circ\prime}$ ($S^{\bullet-}$, 2H+/H_2S) has a similar value (32). Taking the highest occupied molecular orbital (HOMO) energy as an indicator of nucleophilicity for H_2S and HS^-, the corresponding negative values of –9.4 and –7.1 eV determined at the density functional theory level indicate that both species will be prone to react with positively charged metal centers as target electrophiles, but favor the anionic form as a reactive species as the calculations retrieve a higher HOMO energy (8, 13).

Up to date, particularly, the sulfide-ferric heme complexes have been ascribed to transport and storage (33), or to activation and detoxification of sulfide (6, 61). Sulfide-mediated potentially functional processes in mammals have been recognized and described in myeloperoxidase (51), methemoglobin (29, 61), metmyoglobin (6, 29), neuroglobin (57). The present Forum article is focused on the coordination chemistry of inorganic sulfides to iron heme platforms. Herein, both the oxidized and reduced forms of heme-containing proteins, protein mutants, and model compounds, both in organic solvents or under biorelevant conditions that have been explored as targets for sulfide species, are presented to provide a comprehensive description of the outcomes of the interaction of heme iron and sulfide.

The Cases of Binding of Inorganic Sulfide to Ferrous Hemeproteins Are Scarce

The interaction of the HS^- anion with ferrous porphyrinates (Fe^{II}(Por)) in organic media allowed the preparation and characterization of sulfide-bound penta and hexacoordinated, high-spin ferrous compounds with general structures [Fe^{II}(Por)(SH)]$^-$ and [Fe^{II}(Por)$(SH)_2$]$^{2-}$, respectively (52). As nonpolar solvents were used in the experiments, the crown Kryptofix-222 aided the dissolution of the HS^- anion from anhydrous NaHS as source, and is part of the crystal structures. Crystals of the (HS^-) derivatives of Fe^{II}-octaethylporphyrinate (OEP), Fe^{II}(T-p-methoxyphenyl)porphyrinate), and Fe^{II}(T-p-mesityl)porphyrinate) were thus obtained and characterized. Alternatively, $N(Bu)_4SH$ was used as a source of sulfide in organic solvents, and the reaction with a survey of Fe^{II}(5,10,15,20-tetraphenyl porphyrinate [TPP])s yielded the corresponding monosulfide complexes (40). Interestingly, the use of the nonbulky sulfide source allowed the detection of the intermediacy of a bimetallic μ-S complex, for the case of the ferrous octa-fluor-tetraphenylporphyrinate, [$Fe_2(\mu$-SH)$(F_8$-$TPP)_2]^-$. Isolation of a μ-S complex was only attained so far for the case of Ru^{II}(OEP), yielding $Ru_2(\mu$-S)$(OEP)_2$ (14),

and was elusive for the Ga^{III}(TPP) case (41), where metal-centered reduction is inaccessible, suggesting that a reduced form is mandatory for the formation of μ-S-type complexes.

Picket-fence ferrous porphyrinates, sterically impeding the formation of μ-S bridges, were selected to explore the discriminated behavior of the neutral H_2S and the anion HS^-, hampering the acid-base equilibria with the use of organic solvents of different polarities (26). Gaseous H_2S was inert toward ferrous (and also toward the ferric) picket-fence porphyrinates, while the HS^- from $N(Bu)_4SH$ yielded the coordinated $Fe^{II}(SH^-)$ form, regardless of the presence of N-methylimidazole as axial ligand. As this speciation behavior was also observed for the Fe^{II}(TPP), the results suggest an intrinsic inertness of H_2S toward ferrous hemes in organic solvents.

The above results indicate that $Fe^{II}(SH^-)$ porphyrinates can be prepared and isolated in organic media using HS^- but not H_2S, starting from the ferrous systems. As described in the following section, $Fe^{II}(SH^-)$ porphyrinates can also be obtained from the corresponding ferric porphyrinates, after a sulfide-mediated reduction step.

Evidence for the formation of mononuclear ferrous hemeprotein complexes has been reported in the case of myeloperoxidase, where the formation of $Fe^{II}(SH_2)$ in buffered aqueous solutions was proposed from the reaction of sulfide with the ferric form (in the presence of excess sulfide), from the ferrous form, or from the corresponding compounds I and II (25, 51). A rate constant, rate constant for ligand binding (k_{on}) $= 2 \times 10^4\ M^{-1}s^{-1}$, has been reported for the binding of H_2S to the ferrous myeloperoxidase (51).

The binding of sulfide to ferrous myeloperoxidase seems strongly dependent on the nature of the distal amino acids. Based on our observation of the crystal structures of myeloperoxidase, horseradish peroxidase, and lactoperoxidase, the presence of a common distal arginine, absent in hemoglobins, may provide strong stabilization to H_2O molecules in the distal cavity, hampering the access of sulfide ligands. Eventually if sulfide ligands access the distal site, the distal arginine may provide stabilization mechanisms.

Microperoxidase 11 (39), which is a minimalistic heme model compound, derived from the proteolysis of cytochrome c that retains the two thioether linkages of the heme to Cys14 and Cys17, the His18 as fifth ligand, and a water molecule as sixth ligand, represents an opposite example. This heme compound is devoid of distal mechanisms for ligand stabilization (4), and the ferrous form is inert toward sulfide species in the ferrous form.

These dispersed data concerning the interaction of sulfide and ferrous heme systems suggest that the sulfide species are not competing ligands toward O_2, NO, or CO in hemoglobins, while are likely to inhibit the canonical function of myeloperoxidase (51).

The Binding of Inorganic Sulfide to Ferric Heme Compounds Is Observed Mainly in Aqueous Solutions

Compared with the binding of sulfides to ferrous hemes, there is a list of diverse examples of sulfides bound to ferric heme systems, which keeps growing since the pioneer reports on the sulfide-bound ferric hemoglobins from *L. pectinata* (33, 34).

Indeed, up to date, there have been reported more than 40 examples, including hemeproteins, mutants, and heme model compounds, where the binding of inorganic sulfide has been detected and kinetically characterized in aqueous buffered solutions (8). A selection of the collected data is presented in Table 1. In organic solvents, conversely, it has only been reported the formation of a low-spin pentacoordinated ferric heme complex in 1,1,2-trichloroethane (21), later disputed (3). More recently, the intermediacy of an $Fe^{III}(SH^-)$ low-spin form has been detected after the addition of HS^- to two ferric picket-fence model systems only at −80°C in methanol; at room temperature, the fast formation of the metal-centered reduction product was observed (43).

In most of the examples reported in Table 1, the Fe^{III}-sulfide bond formation has been assessed by resonance Raman (4, 48) and/or EPR techniques (6, 51, 61, 65). The complexes are described as hexacoordinated, low-spin ferric structures (46). It can be observed that while the values of k_{on} are all *ca.* 10^4 $M^{-1}s^{-1}$, the values of rate constant for ligand release (k_{off}) are more dispersed. As a consequence, the derived affinity constant (K_{aff}) values ($K_{aff} = k_{on}/k_{off}$) range from 10^3 to $10^9\ M^{-1}$.

The fact that, analytically, the ferric bound sulfides are found as part of the pool of acid-labile sulfur is in line with the higher lability of the neutral form (55). The protonation state of the preferred bound sulfide species has not been addressed spectroscopically under biorelevant conditions so far.

Either H_2S or HS^- Can Bind to Ferric Heme Compounds in Aqueous Solutions if Accessing the Binding Site

In different hemeproteins, the participation of either H_2S or HS^- has been tentatively assumed as reactive (and bound) species, participating in proposed reaction mechanisms. In an attempt to clarify the issue, the rate constant for the binding process has been estimated for different hemeproteins as a function of pH, to envisage the discriminated participation of H_2S or HS^-. Studies of the kinetic behavior of the interaction between ferric hemeproteins and sulfide as a function of pH have been reported for hemoglobins I, II, and III of *L. pectinata* (33), human and porcine hemoglobins (29, 44, 61), myoglobin (6, 8, 29, 44), *Vitreoscilla* hemoglobin (62), and neuroglobin and H64A neuroglobin mutant (57). We included the data in Figure 1, depicting the values of k_{on} of sulfide as a function of pH for the ferric forms of the *L. pectinata* and *Vitreoscilla* hemoglobins, human and porcine hemoglobins, and myoglobin.

As can be observed in Figure 1, the pH intervals ranged from 5.5–6 to 8–9, and the results are coincident, in that the neutral H_2S appears as the fastest reactive species. Furthermore, in the alkaline region, where HS^- is the most abundant species, the reaction rate seems negligible for all the cases reported. This has been assessed for the case of metmyoglobin, where the intrinsic rate constants (k_{int}) for H_2S and HS^- have been estimated retrieving a seemingly null value for the k_{int} (HS^-) (8, 29). It is relevant to address that the pH intervals explored are compromised with the exclusion of other pH-dependent events, affecting the binding within the protein matrices.

According to the above results, it might be tempting to assume that only the neutral H_2S is active for the binding interaction, while the anion HS^- appears as almost inert. To address the issue, a similar experiment using the heme model microperoxidase 11, where the active site is solvent exposed,

Table 1. Literature Data on Kinetic Constants for Sulfide Binding to Ferric Hemeproteins and Heme Model Compounds

Heme compound	*pH,*[a] *temperature*	k_{on} M^{-1} s^{-1}	k_{off} s^{-1}	K_{aff} [b] M^{-1}	*Ref.*
Hemoglobin I, *Lucina pectinata* wild-type	5.5, 20°C	2.26×10^{5}	2.2×10^{-4}[c]	1.0×10^{9}	(33)
Hemoglobin I, *L. pectinata* recombinant	6	2.43×10^{4}	3×10^{-5}	8.1×10^{8}	(36)
Hemoglobin I, *L. pectinata* recombinant, mutant MetE4Val, IleFG4Val	6	6.8×10^{3}	5.5×10^{-5}	1.2×10^{8}	(15)
Hemoglobin I, *L. pectinata* mutant GlnE7Val	6, 25°C	2.76×10^{5}	6×10^{-5}	1.1×10^{9}	(53)
Hemoglobin I, *L. pectinata* mutant GlnE7His	6, 20°C	6.58×10^{4}	—	—	(53)
Hemoglobin I, *L. pectinata* mutant PheB10Leu	6, 20°C	6.17×10^{4}	—	—	(53)
Hemoglobin I, *L. pectinata* mutant PheB10Tyr	6, 20°C	3.9×10^{3}	—	—	(53)
Hemoglobin I, *L. pectinata* mutant PheE11Val	6, 20°C	1.69×10^{4}	—	—	(53)
Hemoglobin I, *L. pectinata* mutant PheE11Tyr	6, 20°C	1.15×10^{4}	—	—	(53)
Hemoglobin I, *L. pectinata* mutant GlnE7Asp	6, 20°C	3.9×10^{4}	1.5×10^{-4}	2.6×10^{8}	(53)
Hemoglobin II, *L. pectinata*	acid limit, 20°C	1.1×10^{4}	1.7×10^{-2}[c]	6.5×10^{5}	(33)
Hemoglobin III, *L. pectinata*	5.5, 20°C	$(4.17–1.06)\times10^{4}$	1.6×10^{-2}[c]	2.6×10^{6}[d]	(33)
Hemoglobin, Vitreoscilla mutant GlnE7Asn	6, 20°C	2.1×10^{5}	1.6×10^{-4}	1.31×10^{9}	(63)
Hemoglobin, Vitreoscilla mutant TyrB10Phe	6, 20°C	1.9×10^{5}	1.9×10^{-4}	1.0×10^{9}	(62)
Hemoglobin, Vitreoscilla wild-type B10Tyr/E7Gln/E11Leu	7, 20°C	6.6×10^{4}	2.5×10^{-4}	4.8×10^{8}	(62)
Hemoglobin, Vitreoscilla mutant TyrB10Ser	6, 20°C	1.6×10^{5}	4.2×10^{-4}	3.8×10^{8}	(63)
Hemoglobin, Vitreoscilla mutant GlnE7Ser	6, 20°C	9×10^{4}	3.6×10^{-4}	2.5×10^{8}	(63)
Hemoglobin, Vitreoscilla mutant GlnE7Tyr	6, 20°C	5×10^{4}	4.5×10^{-4}	1.16×10^{8}	(63)
Hemoglobin, Vitreoscilla mutant LeuE11Phe	6, 20°C	3×10^{4}	3.85×10^{-4}	7.8×10^{7}	(62)
Hemoglobin, Vitreoscilla mutant ProE8Ala	6, 20°C	1.9×10^{4}	2.7×10^{-4}	7×10^{7}	(63)
Hemoglobin, Vitreoscilla mutant TyrB10Ala	6, 20°C	2.5×10^{5}	5.6×10^{-3}	4.5×10^{7}	(63)
Hemoglobin, Vitreoscilla mutant LeuE11Tyr	6, 20°C	1.8×10^{4}	4.8×10^{-4}	3.8×10^{7}	(63)
Hemoglobin, human	7.4, 37°C	$(3.2\pm0.1)\times10^{3}$	$(5.3\pm0.8)\times10^{-2}$	6.0×10^{4}	(61)
Hemoglobin, bovine	7, 20°C	8.5×10^{2}	6.0×10^{-3}	1.4×10^{5}	(44)
Hemoglobin, porcine	6, 20°C	8×10^{3}	0.32	2.5×10^{4}	(62)
Myoglobin, horse heart B10Leu/E7His/E11Val	6, 20°C	1.1×10^{4}	0.55	2×10^{4}	(62)
Myoglobin, horse heart	7, 20°C	7.0×10^{3}	0.54	1.3×10^{4}	(44)
Myoglobin, equine skeletal muscle	7, 25°C	10^{4}	—	—	(8)
Neuroglobin, wild-type	7.4, 25°C	13.8 ± 0.7	$(5.1\pm0.3)\times10^{-3}$	2.7×10^{3}	(57)
Neuroglobin, mutant HisE7Ala	7.4, 25°C	$(58.8\pm3.8)\times10^{3}$	3.7 ± 0.4	1.6×10^{4}	(57)
Myeloperoxidase	7.4, 25°C	$\approx3\times10^{3}$			(51)
Truncated hemoglobin, *Thermobifida fusca* wild type	7, 25°C	5×10^{3}	1.8×10^{-3}	2.8×10^{6}[d]	(48)
Truncated hemoglobin, *T. fusca* triple mutant TyrB10Phe/TyrCD1Phe/TrpG8Phe	7, 25°C	4.4×10^{6}	2.2×10^{-1}	2.0×10^{7}[d]	(48)
Truncated hemoglobin, *T. fusca* mutant TyrB10Phe	7, 25°C	7.8×10^{3}	1.2×10^{-3}	3.1×10^{7}[d]	(48)
Truncated hemoglobin, *T. fusca* mutant TyrCD1Phe	7, 25°C	5.8×10^{3}	1.0×10^{-3}	5.8×10^{6}[d]	(48)
Truncated hemoglobin, *T. fusca* mutant TrpG8Phe	7, 25°C	4.1×10^{4}	3.6×10^{-1}	1.13×10^{5}[d]	(48)
Truncated hemoglobin, Bacillus subtilis	7, 25°C	1.3×10^{4}	2.6×10^{-3}	5.0×10^{6}[d]	(48)
Fe^{III}-Deuterohemin-β-Ala-His	7, 25°C	0.56×10^{4}	8.5	6.89×10^{2}	(66)
Fe^{III}-Deuterohemin-β-Ala-His-Thr	7, 25°C	1.07×10^{4}	8.2	1.31×10^{3}	(66)
Fe^{III}-Deuterohemin-β-Ala-His-Thr-Val	7, 25°C	1.15×10^{4}	8.8	1.31×10^{3}	(66)
Fe^{III}-Deuterohemin-β-Ala-His-Thr-Val-Glu	7, 25°C	2.28×10^{4}	7.5	3.04×10^{3}	(66)
Fe^{III}-Deuterohemin-β-Ala-His-Thr-Val-Glu-Lys	7, 25°C	2.31×10^{4}	7.2	3.21×10^{3}	(66)
Fe^{III}-hemo cyclodextrin complex	7, 25°C	—	—	9.6×10^{4} [e]	(65)
Fe^{III}-N-acetyl microperoxidase 11	6.8, 25°C	2.6×10^{4}	5.7	4.5×10^{3}	(4)
Fe^{III}-N-acetyl microperoxidase 11	7.1, 25°C	1.9×10^{4}	—	—	(8)

[a]Data selected around neutral pH, or closest values reported.
[b]Calculated.
[c]pH 7.5.
[d]Maximum value.
[e]Thermodynamic affinity constant.

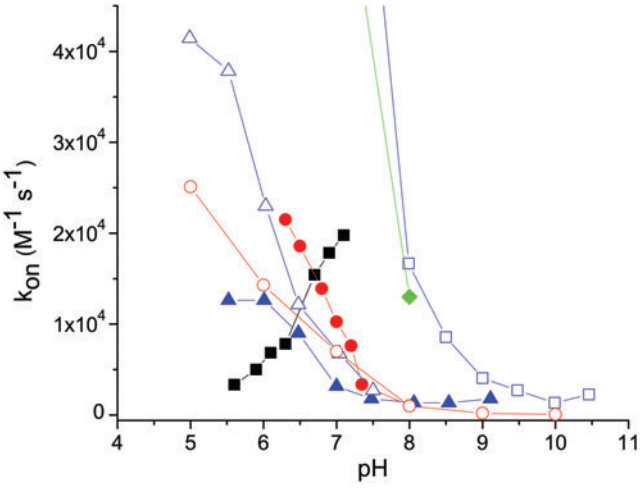

FIG. 1. Reported k_{on} values as a function of pH for microperoxidase 11 (*filled black squares*), metmyoglobin (*filled red circles*), metmyoglobin (*open red circles*), HbI (*open blue squares*), HbII (*filled blue triangles*), and HbIII (*open blue triangles*) of *Lucina pectinata Vitreoscilla* hemoglobin (*filled green rhombus*). Data extracted from Boubeta *et al.* (8), Kraus and Wittenberg (33), Mot *et al.* (44), and Wang *et al.* (62). Color images are available online.

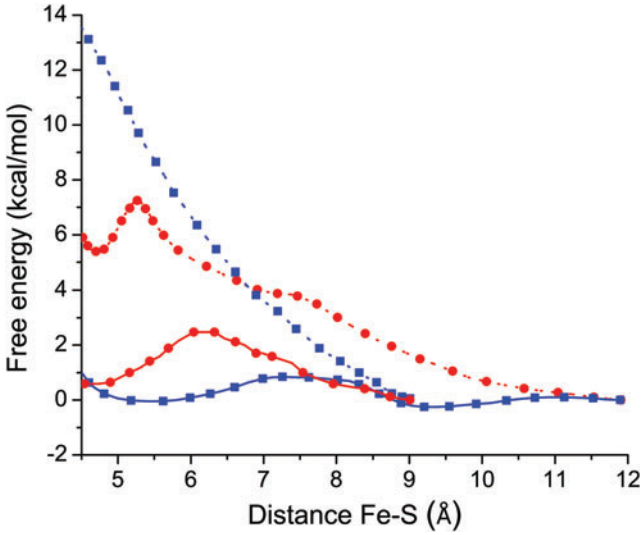

FIG. 2. Free energy profiles for the migration of HS^- (*dotted lines*) and H_2S (*solid lines*) through the E7 tunnel in metmyoglobin (*filled red circles*) and Hb I of *L. pectinata* (*filled blue squares*). Data extracted from Boubeta *et al.* (7, 8). H_2S, hydrogen sulfide; Hb, hemoglobin. Color images are available online.

reveals instead that the anion HS^- is the fastest to bind the ferric heme (Fig. 1), and that the binding of H_2S is also significant, although with a lower intrinsic binding constant. An interpretation at the molecular level of the events describing these results has been attained computationally and is included in the next section (7, 8).

The results suggest that the discriminated behavior of H_2S and HS^- toward ferric heme iron in aqueous solutions cannot be extrapolated either from the observations in organic media or from the analysis of k_{on} *versus* pH for hemeproteins. In contrast with the case of HCN and CN^-, where only the anion is active as binding species regardless of the structural features of the active site and the reaction media (2, 20), for the sulfide species it is mandatory to consider a detailed analysis of the binding mechanism for each species.

Distal Effects Control the Association and Dissociation of Inorganic Sulfide to Ferric Heme Compounds

The association process can be divided into two elementary steps, namely, the ligand migration from the solvent to the distal site, and the formation of the Fe^{III}-sulfide bond. The measurement of the rate-binding constant, k_{on}, encompasses both processes. An observation of the reported values of k_{on} for inorganic sulfide binding (Table 1) suggests a similar binding mechanism operative for the heme compounds listed, as most measurements retrieve a value *ca.* $10^4\ M^{-1}s^{-1}$.

Using classical molecular dynamics (MD) simulations, it has been suggested how the distal effect interactions modulate the association rate of sulfide species to hemeproteins. Specifically, steered MD was used to evaluate the ligand migration free energy profile for H_2S and HS^- for the cases of met-hemoglobin (Hb)I from *L. pectinata* (7), and horse heart metmyoglobin(8) (Fig. 2). Altogether, these results were interpreted in terms of the high desolvation requirement of the charged HS^- during the migration process from the bulk to the distal cavity, responsible for the specific selectivity of these hemeproteins for the neutral H_2S. The computational evaluation for the migration step of the binding process is in agreement with the tendency of k_{on} as a function of pH reported for both cases (6, 8, 29, 33). Thus, MD assists the interpretation of the role of pH in the binding of sulfide species to hemeproteins, suggesting that the binding is seemingly null for the anionic form only due to its impossibility to access the binding site, and not as a consequence of a weaker reactivity. Significantly, for the case of microperoxidase 11, the absence of a protein matrix accounts for the significant reactivity of HS^- and H_2S, due to lack of restrictions for access to the binding site (8). The binding mechanism of the anion HS^- to the microperoxidase model compound, intuitively favored by its higher nucleophilicity (8), deserves further research for a proper description of the reaction mechanism.

The binding of small ligands to ferric hemeproteins is hampered by a coordinated water molecule. The value of k_{on} *ca.* $10^4\ M^{-1}s^{-1}$ (Table 1) systematically observed for ferric hemeproteins reports the sole binding of H_2S, and can be tentatively explained in terms of a dissociative mechanism involving the water molecule coordinated to the distal position. In fact, a simple Eyring analysis shows that the release of the coordinated water molecule ($k_{off}(H_2O) \approx 10^4\ s^{-1}$) retrieves a value of $\Delta G^{\neq}$ of *ca.* 12 kcal/mol, which is consistent with the interaction free energy of a water molecule coordinating with a ferric porphyrin system (11, 50).

A more detailed analysis should take into consideration the interactions of the coordinated water molecule with the surrounding amino acids, expected to affect the value of k_{on}. Indeed, those interactions probably explain the special cases among the reported data (Table 1), where specific mutations

on the distal side affect the value of k_{on} within one order of magnitude, at the most. For example, the GlnE7Val and PheB10Tyr mutants of met-HbI of *L. pectinata* show an increase and a decrease of one order of magnitude of k_{on}, respectively. With the E7 mutation, the water molecule is destabilized, but the inclusion of a TyrB10 as a distal amino acid may provide further stabilization to the coordinated water molecule (53). Other E7 mutations that still provide stabilization through hydrogen bonding to the coordinated water molecule (GlnE7Asn or GlnE7His) do not modify the k_{on} value significantly, when compared with the wild type. The k_{on} results for these mutations suggest that the E7 position might not be acting as a gate, and highlight the role of stabilization of the coordinated water molecule in ferric hemeproteins, contrasting with the analysis of ferrous systems.

Additional evidence of the variation of k_{on} as a function of distal mechanisms stabilizing the coordinated water molecule has been provided by mutations on the truncated hemoglobin O of *Thermobifida fusca* (trHbO). Similar to the case of HbI mutants, the mutations of H bond donor residues by phenylalanine residues reflect an increased value of k_{on} from one to three orders of magnitude of k_{on}, depending on the number of mutated residues (Table 1) (48, 49).

In this context, it can be speculated that the anomalous case of ferric horseradish peroxidase, which is inert toward sulfide species at neutral pH, can be explained in terms of a strong stabilization of the coordinated water molecule by a distal positively charged arginine residue.

As a general conclusion, it can be derived that the dispersed k_{on} values for the binding of O_2, NO, or CO to ferrous hemeproteins, devoid of a sixth ligand, are a consequence of a combination between the distinct interactions of the ligands while migrating from the bulk to the distal site, and eventually the requirement of the displacement of water molecules stabilized by the distal amino acids near the metal center (10). Conversely, for the case of the ferric hemeprotein, the rate-limiting step is the release of a coordinated water molecule, rendering a low fluctuation in the k_{on} values for the binding of sulfide species.

The stabilization of bound sulfide species was first addressed in the paradigmatic HbI of *L. pectinata*, where the elevated content of aromatic amino acids in the distal site (3 × phenylalanine) was presumed to impose a hydrophobic environment, favoring the stabilization of neutral H_2S as a coordinated ligand (53).

The pK_a shift between free and coordinated H_2S can be roughly compared with the pK_a shifts observed for H_2O in ferric hemeproteins. Taking into consideration that the pK_a of the bulk water is about 14, experimental and computational results show that the pK_a shift between the bulk H_2O and the coordinated H_2O is $\approx$4 pK_a units (9, 33, 38, 58). Using the same assumptions, and considering that the pK_a of H_2S in aqueous solutions is $\approx$7, this analysis suggests that the coordinated H_2S is deprotonated at physiological pH. This is in agreement with the reported quantum mechanics/molecular mechanics (QM/MM) energy profile evaluating the energy cost for the deprotonation step, suggesting that the coordinated H_2S spontaneously deprotonates to give HS^-, with a ΔE value of *ca.* −12 kcal/mol for HbI of *L. pectinata*, assisted either by GlnE7 or by the entrance of water molecules to the active site (Fig. 3) (7).

As detailed for the stabilization of the coordinated water molecule, the stabilization of the HS^- ligand can also be explained in terms of distal hydrogen bonding interactions, and is reported by the values of k_{off} (Table 1). Evidence of this interaction can be also obtained from MD simulations. Figure 4 shows the snapshots taken from the reported MD simulations for the HS^- complexes of HbI of *L. pectinata* (left panel) (7), and the truncated hemoglobin from trHbO of *T. fusca* (right panel) (48).

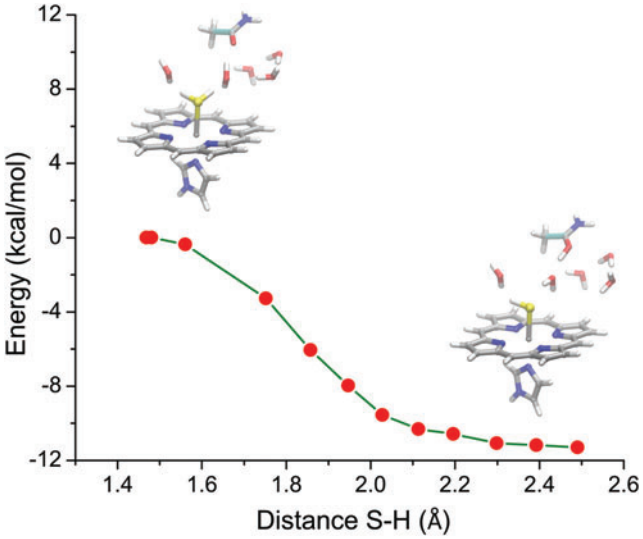

FIG. 3. QM/MM energy profile for the deprotonation of the low-spin Fe^{III}-SH_2 complex in HbI of *L. pectinata*. The reaction coordinate is de S-H distance. Data extracted from Boubeta *et al.* (7). QM/MM, quantum mechanics/molecular mechanics. Color images are available online.

Following a similar analysis for the case of neuroglobin, the 700-fold higher k_{off} value observed for sulfide for the His64Ala mutant compared with wild-type neuroglobin is consistent with the role of distal histidine residue in stabilizing sulfide (57). In addition, single mutations on trHbO of *T. fusca* dramatically affect the stabilization of the coordinated HS^- ligand, with an $\sim$300-fold increase in the k_{off} for the TrpG8Phe mutant (48). The value of k_{off} for microperoxidase 11 (Table 1), the highest reported so far, is explained in this context by the absence of distal effects.

A global reaction mechanism derived from the experimental and theoretical analysis is presented in Figure 5. The first step encompasses the release of the coordinated water molecule, interpreted as a rate-limiting step after the analysis of the k_{on} values included in Table 1. As HS^- is excluded by the protein matrix as a consequence of its high desolvation cost, only the neutral H_2S is available for the binding step. After coordination, a barrierless deprotonation step, and surrounding water molecules or distal amino acids act as proton acceptors. The HS^- bound ligand is finally stabilized by hydrogen bonding interactions with distal amino acids.

The Role of the Proximal Ligand in the Stabilization of Coordinated Sulfide to Ferric Hemeproteins is Evidenced in Models Devoid of Distal Interactions

The absence of a nitrogen containing ligand in the fifth coordination position of ferric porphyrinates drives the addition of sulfide to the fast formation of the metal-centered

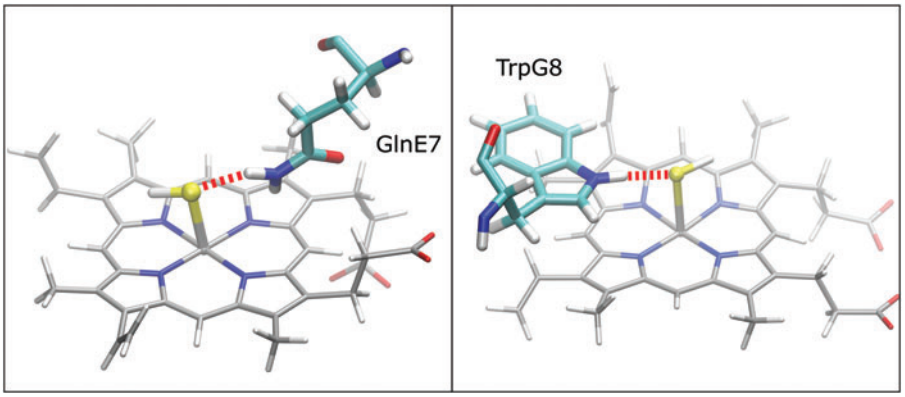

FIG. 4. Stabilization of the coordinated HS^- during the MD simulations for the binding of sulfide to ferric hemeproteins. *Left panel*: Stabilization of HS^- ligand by GlnE7 of HbI of *L. pectinata*. *Right panel*: Stabilization of HS^- ligand by TrpG8 of trHbO of *T. fusca*. Data extracted from Boubeta *et al.* (7) and Nicoletti *et al.* (48). MD, molecular dynamics; trHbO, truncated hemoglobin O of *Thermobifida fusca.* Color images are available online.

reduction product (43). Conversely, the presence of nitrogen containing bases as proximal ligands reveals that complexes with varied stability can be prepaired. The release constant, k_{off}, has been determined in many cases, and values of k_{off} spanned within six orders of magnitude (from 10^{-5} to $10\,s^{-1}$, Table 1), with an impact in the kinetically derived $K_{aff} = k_{on}/k_{off}$.

To discriminate the proximal contribution to sulfide affinity of ferric heme compounds, the binding has been reported, at least, in three diverse model compounds sharing as common features a nitrogen containing fifth ligand, and structurally hampered, or even unavailable, distal mechanisms for ligand stabilization.

Using microperoxidase 11, the moderately stable binding of inorganic sulfide was observed, and the complex was characterized by means of resonance Raman and UV-Vis spectroscopies (4). To assess the opportunities of the amino acidic residues for the stabilization of sulfide species as ligands, the system was studied by means of MD simulations, which suggested that none of the amino acidic residues interacted with coordinated HS^-, and thus, the $Fe^{III}(SH^-)$ complex is solvent exposed (Fig. 6A). Furthermore, the results suggested that a conformation involving the interaction of the H atom of the N_δ of the proximal histidine with the carbonyl group of the Thr19 was significantly populated (Fig. 6B), with the consequent change in charge distribution around the heme center (4). The maximum population is centered around 2 Å, suggesting a H bonded interaction. The kinetic study of the binding of inorganic sulfide at neutral pH revealed that the k_{on} value was similar to that of most of the native hemeproteins studied (Table 1), while the k_{off} was increased, thus retrieving a value of K_{aff} in the lower limit of those reported so far (8). Significantly, the case highlighted the isolated role of the proximal amino acid in the stabilization of the Fe^{III}-sulfide complex.

This computational description of the proximal side has been experimentally verified in a series of heme b type model compounds, namely, a series of deuterohemin-His-peptides, where the binding of sulfide was evaluated in the presence of an increasing number of proximal interactions with the N_δ of the coordinated histidine (66). The k_{on} value showed an increase of half an order of magnitude when allowing one H

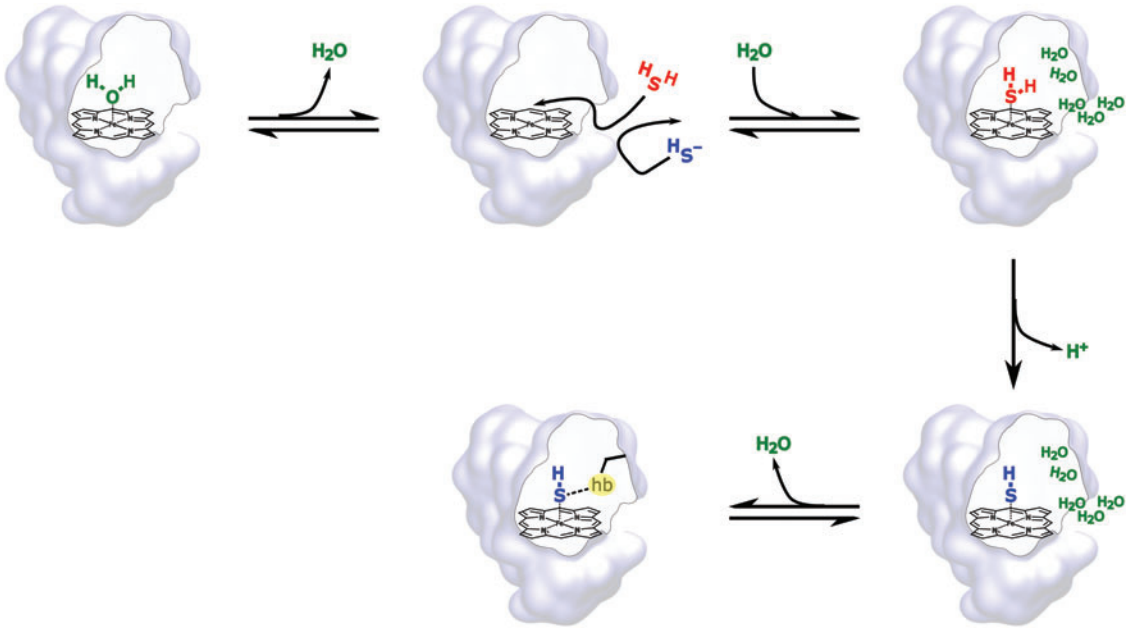

FIG. 5. Proposed global reaction mechanism for the binding of sulfide species to ferric hemeproteins. Data extracted from Boubeta *et al.* (7). Color images are available online.

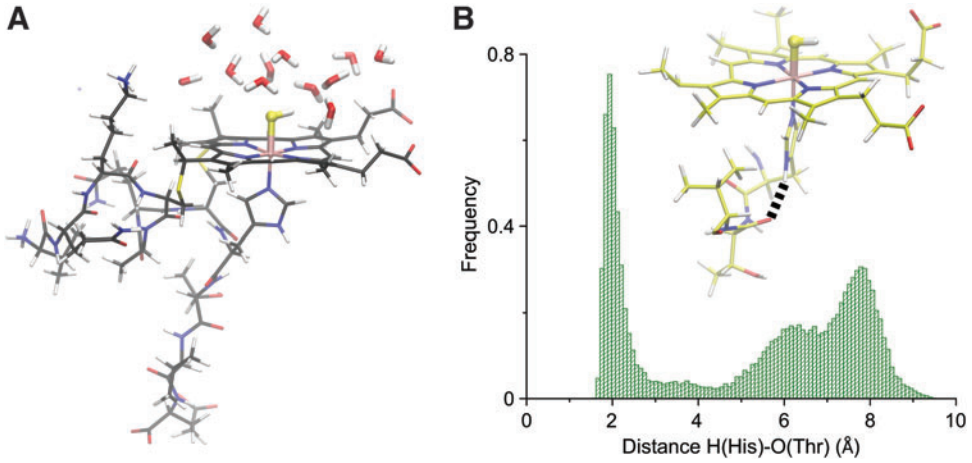

FIG. 6. Binding of sulfide to the ferric microperoxidase 11 model compound. (A) Representative structure for the sulfide complex of ferric microperoxidase 11, obtained from the MD simulations. **(B)** Hydrogen-bonding interaction between the N_δ of the proximal histidine and the carbonyl group of Thr19 of the amino acidic chain, and histogram showing the distribution of distance HN_δ(Im)–O(Thr19) along the MD trajectory. Data extracted from Bieza *et al.* (4). Im, imidazole. Color images are available online.

bonding interaction with the peptide backbone (N_δ-Thr), and an additional increase in one order of magnitude when including a second interaction (N_δ-Thr and N_δ-Glu). In parallel, the k_{off} values for the binding of sulfide to these deuterohemin derivatives were unchanged after the inclusion of the N_δ-Thr interaction, but decreased in the addition of the N_δ-Glu interaction. As a consequence, the kinetically derived K_{aff} showed an increase only as a result of the participation of one or two hydrogen bonding interactions of the amino acid backbone with the Nδ of the coordinated histidine to the Fe^{III}, in the absence of distal stabilization mechanisms.

Additional evidence for the discriminated role of the proximal ligand was provided by the use of a 1:1 inclusion complex of a water soluble iron porphyrinate, namely Fe^{III}(5,10,15,20-tetrakis(4-sulfonatophenyl)porphyrinate), in a methylated β-cyclodextrin (CD) dimer, linked *via* a pyridine ligand (65). These systems, called methemo CDs or methemoCDs, have been characterized and used to mimic hemeproteins in aqueous solutions, and provide a hydrophobic environment in the surroundings of the binding site. The thermodynamic K_{aff} was reported and is slightly favored compared with the water-exposed active sites of the two models presented above.

Interestingly, the reactivity of the ferric sulfide complex of met-hemoCD was evaluated toward CO and O_2, and showed the formation of the corresponding ferrous hexacoordinated complexes, with the release of thiyl radicals, suggesting that the $Fe^{II}(SH^\bullet)$ resonant structure is crucial to interpret the reactivity of the complex (65). Particularly, it is interesting to address that the interaction with O_2 mimics the initial step of the catalytic oxidative decomposition of sulfides, described for methemoglobin and metmyoglobin (6, 29, 61).

Sulfide-Bound Species Initiate the Metal-Centered Reduction of Hemeproteins

The experiments of binding of inorganic sulfide to ferric hemeproteins under anaerobic conditions reveal the final formation of the ferrous form and sulfur; the kinetics of the process varies significantly in the different systems (42, 51, 53, 61).

Using methanol as solvent of hemeprotein models devoid of a proximal ligand, a fast reduction has been reported, and by lowering the temperature at −80°C the intermediacy of coordinated sulfide was detected. The reduction product is formed after the cleavage of an $Fe^{III}(SH^-)$ form forming thiyl radical ($HS^\bullet$), as demonstrated by trapping experiments using a radical trap as 5,5-dimethyl-1-pyrroline N-oxide (43). The experimental result reveals that the resonance form $Fe^{II}(SH^\bullet)$ represents a significant contribution to the reactant moiety. Experimental evidence of the relevance of the resonance structure $Fe^{II}(SH^\bullet)$ was also provided by experiments on the met-hemoCD complex with CO and O_2 (65).

Under biorelevant conditions, up to date, the reduction mechanisms on hemeproteins have only been hypothesized. A comparative reduction tendency for a series of mutants of the HbI of *L. pectinata* was suggested to be governed by a strong dependence on the proton acceptor amino acids in the distal side (53). This analysis considers that hemeproteins with low-polarity distal amino acids form stable ferric-SH_2 heme species, and sulfide release is dictated by low H_2S dissociation without inducing a significant metal-centered reduction. The presence of strong proton acceptor groups, in contrast, was suggested to explain the metal-centered reduction. Mechanistically, the Fe^{III}/Fe^{II} reduction was suggested to be favored after the rapid deprotonation of the bound H_2S species, forming the reactive Fe^{II}-$SH^\bullet$ species, in turn reacting with a second H_2S molecule (53, 54).

However, if this were the case, the ferric heme model compounds devoid of a distal cavity that carry a solvent-exposed ligated sulfide species would be prone to fast reduction (4, 65, 66). Indeed, the complexes have a lifetime of hours, regardless of the potential role of surrounding water molecules acting as proton acceptors. In addition, our computational results on the wild-type HbI of *L. pectinata* suggest that the first deprotonation of the preferred bound species is quickly assisted by water molecules or distal amino acid rearrangements induced by the concomitant formation of

$Fe^{III}(SH_2)$. Further QM/MM calculations showed that the deprotonation step is barrierless, yielding $Fe^{III}(SH^-)$ (7). Thus, the deprotonation of $Fe^{III}(SH_2)$ does not seem to participate as a rate-limiting step; the analysis for the formation of the metal-centered reduction product should be commenced after the formation of the bound species HS^-. Rationalized in terms of the resonance forms $Fe^{III}(SH^-)$/$Fe^{II}(SH^{\bullet})$. In accordance with this analysis, a mechanistic proposal for the metal-centered reduction mediated by sulfide has been presented for the case of myeloperoxidase, and suggests the release of the thiyl radical (51). The Fe-S bond cleavage appears as a plausible rate-limiting step for the process in agreement with the timescales experimentally observed. Interestingly, Jensen and Fago recently reported on the role of stoichiometry on the timescale of the reduction process for metmyoglobin and methemoglobin (29). This contribution sums up to the above-reported analysis for the description of the reduction mechanism of hemeproteins mediated by sulfide. Still, the molecular determinants of the metal-centered reduction of hemeproteins mediated by inorganic sulfide are not completely elucidated and deserve further inspection.

Unresolved Problems

Recent research elucidating the biochemical relevance of the interaction of sulfide and hemeproteins highlights the role of this chemical process. Intrinsic features of the H_2S molecule—acid-base equilibria, redox equilibria, and formation of polysulfides—disclose different levels of complexity when attempting to describe the molecular determinants of the interaction. The analysis of the protonation state of the sulfide species bound to ferric hemes has not been assessed experimentally so far, probably limited by both difficulties in sulfur atom enrichment and by spectroscopic constraints of the Fe-S bond and sulfide-bound exchangeable protons.

Most of the cases in the literature describe the interaction of sulfide with ferric hemoglobins, with a deep insight on the hemoglobins of the clam *L. pectinata*, different metmyoglobins and methemoglobins, and the description of the interaction has been enriched by a combination of spectroscopic methods, experiments with mutants or model compounds, and computational experiments. The interaction of sulfide with peroxidases has been reported for the mammalian peroxidases, especially for the myeloperoxidase, but the molecular details of the interaction remain to be elucidated.

Concluding Remarks

The coordination chemistry of sulfide and hemeproteins, and the activation of sulfide by hemeproteins, is expected to be involved in biorelevant processes as the reaction with O_2 forming sulfur oxygen reactive species, formation of sulfheme compounds, the cross talk with NO or CO, and formation of disulfide or polysulfides. Herein, we attempted to present the state of the art in the interaction of sulfide species with hemeproteins in the ferrous and ferric oxidation states, providing a picture of the occurrence and an analysis of the kinetic descriptors of the binding. The interaction of sulfides and the heme iron should be taken into consideration when interpreting sulfide biochemistry, signaling, and pharmacology, along with the reactions with proteins or low-molecular-weight thiols.

Funding Information

This work was supported by grants from Universidad de Buenos Aires (UBACYT 20020170100043BA), Agencia Nacional de Promoción Científica y Tecnológica (PICT 2014-1022, PICT 2015-2761), and Consejo Nacional de Promoción Científica y Técnica (11220150100303CO, 1122015010039 4CO).

References

1. Abe K and Kimura H. The possible role of hydrogen sulfide as an endogenous neuromodulator. *J Neurosci* 16: 1066–1071, 1996.
2. Ascenzi P, Sbardella D, Santucci R, and Coletta M. Cyanide binding to ferrous and ferric microperoxidase-11. *J Biol Inorg Chem* 21: 511–522, 2016.
3. Balch AL, Cornman CR, Safari N, and Latos-Grazynski L. Proton NMR studies of the reduction of paramagnetic iron(III) alkyl porphyrin complexes to diamagnetic iron(II) alkyl complexes. *Organometallics* 9: 2420–2421, 1990.
4. Bieza SA, Boubeta F, Feis A, Smulevich G, Estrin DA, Boechi L, and Bari SE. Reactivity of inorganic sulfide species toward a heme protein model. *Inorg Chem* 54: 527–533, 2015.
5. Bolden C, King SB, and Kim-Shapiro DB. Reactions between nitrosopersulfide and heme proteins. *Free Radic Biol Med* 99: 418–425, 2016.
6. Bostelaar T, Vitvitsky V, Kumutima J, Lewis BE, Yadav PK, Brunold TC, Filipovic M, Lehnert N, Stemmler TL, and Banerjee R. Hydrogen sulfide oxidation by myoglobin. *J Am Chem Soc* 138: 8476–8488, 2016.
7. Boubeta FM, Bari SE, Estrin DA, and Boechi L. Access and binding of H_2S to hemeproteins: the Case of HbI of *Lucina pectinata*. *J Phys Chem B* 120: 9642–9653, 2016.
8. Boubeta FM, Bieza SA, Bringas M, Estrin DA, Boechi L, and Bari SE. Mechanism of sulfide binding by ferric hemeproteins. *Inorg Chem* 57: 7591–7600, 2018.
9. Brunori M, Amiconi G, Antonini E, Wyman J, Zito R, and Rossi Fanelli A. The transition between 'acid' and 'alkaline' ferric heme proteins. *Biochim Biophys Acta* 154: 315–322, 1968.
10. Bustamante JP, Szretter ME, Sued M, Martí MA, Estrin DA, and Boechi L. A quantitative model for oxygen uptake and release in a family of hemeproteins. *Bioinformatics* 32: 1805–1813, 2016.
11. Cao W, Christian JF, Champion PM, Rosca F, and Sage JT. Water penetration and binding to ferric myoglobin. *Biochemistry* 40: 5728–5737, 2001.
12. Capece L, Boechi L, Perissinotti LL, Arroyo-Mañez P, Bikiel DE, Smulevich G, Marti MA, and Estrin DA. Small ligand–globin interactions: reviewing lessons derived from computer simulation. *Biochim Biophys Acta* 1834: 1722–1738, 2013.
13. Chai J-D and Head-Gordon M. Long-range corrected hybrid density functionals with damped atom–atom dispersion corrections. *Phys Chem Chem Phys* 10: 6615, 2008.
14. Chatwin SL, Diggle RA, Jazzar RFR, Macgregor SA, Mahon MF, and Whittlesey MK. Structure, reactivity, and computational studies of a novel ruthenium hydrogen sulfide dihydride complex. *Inorg Chem* 42: 7695–7697, 2003.
15. Collazo E, Pietri R, De Jesús W, Ramos C, Del Toro A, León RG, Cadilla CL, and López-Garriga J. Functional characterization of the purified holo form of hemoglobin I from *Lucina pectinata* overexpressed in *Escherichia coli*. *Protein J* 23: 239–245, 2004.

16. Cooper CE and Brown GC. The inhibition of mitochondrial cytochrome oxidase by the gases carbon monoxide, nitric oxide, hydrogen cyanide and hydrogen sulfide: chemical mechanism and physiological significance. *J Bioenerg Biomembr* 40: 533–539, 2008.
17. Cortese-Krott MM, Koning A, Kuhnle GGC, Nagy P, Bianco CL, Pasch A, Wink DA, Fukuto JM, Jackson AA, van Goor H, Olson KR, and Feelisch M. The reactive species interactome: evolutionary emergence, biological significance, and opportunities for redox metabolomics and personalized medicine. *Antioxid Redox Signal* 27: 684–712, 2017.
18. Cortese-Krott MM, Kuhnle GGC, Dyson A, Fernandez BO, Grman M, DuMond JF, Barrow MP, McLeod G, Nakagawa H, Ondrias K, Nagy P, King SB, Saavedra JE, Keefer LK, Singer M, Kelm M, Butler AR, and Feelisch M. Key bioactive reaction products of the NO/H_2S interaction are S/N-hybrid species, polysulfides, and nitroxyl. *Proc Natl Acad Sci U S A* 112: E4651–E4660, 2015.
19. Cuevasanta E, Denicola A, Alvarez B, and Möller MN. Solubility and permeation of hydrogen sulfide in lipid membranes. *PLoS One* 7: e34562, 2012.
20. Dou Y, Olson JS, Wilkinson AJ, and Ikeda-Saito M. Mechanism of hydrogen cyanide binding to myoglobin. *Biochemistry* 35: 7107–7113, 1996.
21. English DR, Hendrickson DN, Suslick KS, Eigenbrot CW, and Scheidt WR. Low-spin five-coordinate ferric porphyrin complex: [5, 10, 15, 20-tetrakis(4-methoxyphenyl)porphyrinato](hydrosulfido)iron(III). *J Am Chem Soc* 106: 7258–7259, 1984.
22. Filipovic MR. Persulfidation (S-sulfhydration) and H2S. In: *Chemistry, Biochemistry and Pharmacology of Hydrogen Sulfide*, edited by Moore PK and Whiteman M. Cham, Switzerland: Springer International Publishing, 2015, pp. 29–59.
23. Filipovic MR, Miljkovic JL, Nauser T, Royzen M, Klos K, Shubina T, Koppenol WH, Lippard SJ, and Ivanović-Burmazović I. Chemical characterization of the smallest *S*-Nitrosothiol, HSNO; cellular cross-talk of H_2S and *S*-Nitrosothiols. *J Am Chem Soc* 134: 12016–12027, 2012.
24. Fukuto JM, Carrington SJ, Tantillo DJ, Harrison JG, Ignarro LJ, Freeman BA, Chen A, and Wink DA. Small molecule signaling agents: the integrated chemistry and biochemistry of nitrogen oxides, oxides of carbon, dioxygen, hydrogen sulfide, and their derived species. *Chem Res Toxicol* 25: 769–793, 2012.
25. Garai D, Ríos-González BB, Furtmüller PG, Fukuto JM, Xian M, López-Garriga J, Obinger C, and Nagy P. Mechanisms of myeloperoxidase catalyzed oxidation of H_2S by H_2O_2 or O_2 to produce potent protein Cys-polysulfide-inducing species. *Free Radic Biol Med* 113: 551–563, 2017.
26. Hartle MD, Prell JS, and Pluth MD. Spectroscopic investigations into the binding of hydrogen sulfide to synthetic picket-fence porphyrins. *Dalton Trans* 45: 4843–4853, 2016.
27. Huang CW and Moore PK. H2S synthesizing enzymes: biochemistry and molecular aspects. In: *Chemistry, Biochemistry and Pharmacology of Hydrogen Sulfide*, edited by Moore PK and Whiteman M. Cham, Switzerland: Springer International Publishing, 2015, pp. 3–25.
28. Hughes MN, Centelles MN, and Moore KP. Making and working with hydrogen sulfide. *Free Radic Biol Med* 47: 1346–1353, 2009.
29. Jensen B and Fago A. Reactions of ferric hemoglobin and myoglobin with hydrogen sulfide under physiological conditions. *J Inorg Biochem* 182: 133–140, 2018.
30. Kabil O and Banerjee R. Enzymology of H_2S biogenesis, decay and signaling. *Antioxid Redox Signal* 20: 770–782, 2014.
31. Kimura H. Hydrogen sulfide and polysulfide signaling. *Antioxid Redox Signal* 27: 619–621, 2017.
32. Koppenol WH and Bounds PL. Signaling by sulfur-containing molecules. Quantitative aspects. *Arch Biochem Biophys* 617: 3–8, 2017.
33. Kraus DW and Wittenberg JB. Hemoglobins of the *Lucina pectinata*/bacteria symbiosis. I. Molecular properties, kinetics and equilibria of reactions with ligands. *J Biol Chem* 265: 16043–16053, 1990.
34. Kraus DW, Wittenberg JB, Lu JF, and Peisach J. Hemoglobins of the *Lucina pectinata*/bacteria symbiosis. II. An electron paramagnetic resonance and optical spectral study of the ferric proteins. *J Biol Chem* 265: 16054–16059, 1990.
35. Kuang Q, Xue N, Chen J, Shen Z, Cui X, Fang Y, and Ding X. Low plasma hydrogen sulfide is associated with impaired renal function and cardiac dysfunction. *Am J Nephrol* 47: 361–371, 2018.
36. León RG, Munier-Lehmann H, Barzu O, Baudin-Creuza V, Pietri R, López-Garriga J, and Cadilla CL. High-level production of recombinant sulfide-reactive hemoglobin I from *Lucina pectinata* in *Escherichia coli*. *Protein Expr Purif* 38: 184–195, 2004.
37. Li Q and Lancaster JR. Chemical foundations of hydrogen sulfide biology. *Nitric Oxide* 35: 21–34, 2013.
38. Marques H and Perry C. Hemepeptide models for hemoproteins: the behavior of -acetylmicroperoxidase-11 in aqueous solution. *J Inorg Biochem* 75: 281–291, 1999.
39. Marques HM. Insights into porphyrin chemistry provided by the microperoxidases, the haempeptides derived from cytochrome c. *Dalton Trans* 4371, 2007.
40. Meininger DJ, Arman HD, and Tonzetich ZJ. Synthesis, characterization, and binding affinity of hydrosulfide complexes of synthetic iron(II) porphyrinates. *J Inorg Biochem* 167: 142–149, 2017.
41. Meininger DJ, Chee-Garza M, Arman HD, and Tonzetich ZJ. Gallium(III) tetraphenylporphyrinates containing hydrosulfide and thiolate ligands: structural models for sulfur-bound Iron(III) hemes. *Inorg Chem* 55: 2421–2426, 2016.
42. Mishanina TV, Libiad M, and Banerjee R. Biogenesis of reactive sulfur species for signaling by hydrogen sulfide oxidation pathways. *Nat Chem Biol* 11: 457–464, 2015.
43. Mittra K, Singha A, and Dey A. Mechanism of Reduction of Ferric Porphyrins by Sulfide: identification of a Low Spin Fe^{III}–SH Intermediate. *Inorg Chem* 56: 3916–3925, 2017.
44. Mot AC, Bischin C, Damian G, Attia AAA, Gal E, Dina N, Leopold N, and Silaghi-Dumitrescu R. Fe(III)—sulfide interaction in globins: characterization and quest for a putative Fe(IV)-sulfide species. *J Inorg Biochem* 179: 32–39, 2018.
45. Mustafa AK, Gadalla MM, and Snyder SH. Signaling by gasotransmitters. *Sci Signal* 2: re2, 2009.
46. Nicholls P. The formation and properties of sulphmyoglobin and sulphcatalase. *Biochem J* 81: 374–383, 1961.
47. Nicholls P, Marshall DC, Cooper CE, and Wilson MT. Sulfide inhibition of and metabolism by cytochrome *c* oxidase. *Biochem Soc Trans* 41: 1312–1316, 2013.
48. Nicoletti FP, Comandini A, Bonamore A, Boechi L, Boubeta FM, Feis A, Smulevich G, and Boffi A. Sulfide binding properties of truncated hemoglobins. *Biochemistry* 49: 2269–2278, 2010.

49. Nicoletti FP, Droghetti E, Howes BD, Bustamante JP, Bonamore A, Sciamanna N, Estrin DA, Feis A, Boffi A, and Smulevich G. H-bonding networks of the distal residues and water molecules in the active site of *Thermobifida fusca* hemoglobin. *Biochim Biophys Acta* 1834: 1901–1909, 2013.
50. Ostrich IJ, Liu G, Dodgen HW, and Hunt JP. Oxygen-17 nuclear magnetic resonance study of water exchange on water-soluble iron(III) porphyrins. *Inorg Chem* 19: 619–621, 1980.
51. Pálinkás Z, Furtmüller PG, Nagy A, Jakopitsch C, Pirker KF, Magierowski M, Jasnos K, Wallace JL, Obinger C, and Nagy P. Interactions of hydrogen sulfide with myeloperoxidase: sulfide is a substrate and inhibitor of myeloperoxidase. *Br J Pharmacol* 172: 1516–1532, 2015.
52. Pavlik JW, Noll BC, Oliver AG, Schulz CE, and Scheidt WR. Hydrosulfide (HS^-) coordination in iron porphyrinates. *Inorg Chem* 49: 1017–1026, 2010.
53. Pietri R, Lewis A, León RG, Casabona G, Kiger L, Yeh S-R, Fernandez-Alberti S, Marden MC, Cadilla CL, and López-Garriga J. Factors controlling the reactivity of hydrogen sulfide with hemeproteins. *Biochemistry* 48: 4881–4894, 2009.
54. Pietri R, Román-Morales E, and López-Garriga J. Hydrogen sulfide and hemeproteins: knowledge and mysteries. *Antioxid Redox Signal* 15: 393–404, 2011.
55. Predmore BL, Lefer DJ, and Gojon G. Hydrogen sulfide in biochemistry and medicine. *Antioxid Redox Signal* 17: 119–140, 2012.
56. Riahi S and Rowley CN. Why can hydrogen sulfide permeate cell membranes? *J Am Chem Soc* 136: 15111–15113, 2014.
57. Ruetz M, Kumutima J, Lewis BE, Filipovic MR, Lehnert N, Stemmler TL, and Banerjee R. A distal ligand mutes the interaction of hydrogen sulfide with human neuroglobin. *J Biol Chem* 292: 6512–6528, 2017.
58. Sun J, Wilks A, Ortiz de Montellano PR, and Loehr TM. Resonance Raman and EPR spectroscopic studies on heme-heme oxygenase complexes. *Biochemistry* 32: 14151–14157, 1993.
59. Sun W, Nešić S, Young D, and Woollam RC. Equilibrium expressions related to the solubility of the sour corrosion product mackinawite. *Ind Eng Chem Res* 47: 1738–1742, 2008.
60. Szabo C and Papapetropoulos A. International union of basic and clinical pharmacology. CII: pharmacological modulation of H_2S Levels: H_2S donors and H_2S Biosynthesis Inhibitors. *Pharmacol Rev* 69: 497–564, 2017.
61. Vitvitsky V, Yadav PK, Kurthen A, and Banerjee R. Sulfide oxidation by a noncanonical pathway in red blood cells generates thiosulfate and polysulfides. *J Biol Chem* 290: 8310–8320, 2015.
62. Wang D, Liu L, Wang H, Xu H, Chen L, Ma L, and Li Z. Clues for discovering a new biological function of *Vitreoscilla* hemoglobin in organisms: potential sulfide receptor and storage. *FEBS Lett* 590: 1132–1142, 2016.
63. Wang D, Wang H, Li H, Liu L, and Li Z. Studies on the contributions of steric and polarity effects to the H2S-binding properties of Vitreoscilla hemoglobin. *J Mol Struct* 1128: 300–306, 2017.
64. Wang R. Two's company, three's a crowd: can H_2S be the third endogenous gaseous transmitter? *FASEB J* 16: 1792–1798, 2002.
65. Watanabe K, Suzuki T, Kitagishi H, and Kano K. Reaction between a haemoglobin model compound and hydrosulphide in aqueous solution. *Chem Commun* 51: 4059–4061, 2015.
66. Zhao Z, Wang D, Wang M, Sun X, Wang L, Huang X, Ma L, and Li Z. Proximal environment controlling the reactivity between inorganic sulfide and heme-peptide model. *RSC Adv* 6: 78858–78864, 2016.

Address correspondence to:
Dr. Sara Elizabeth Bari
Instituto de Química Física de los Materiales, Medio Ambiente y Energía. (INQUIMAE) CONICET
Universidad de Buenos Aires
Intendente Güiraldes 2160
Pabellón 2, Piso 3
Buenos Aires C1425EGA
Argentina

E-mail: bari@qi.fcen.uba.ar

Date of first submission to ARS Central, September 12, 2019; date of acceptance, September 17, 2019.

Abbreviations Used

3-MST = 3-mercaptopyruvil sulfuryl transferase
ca. = approximately
CD = cyclodextrin
CO = carbon monoxide
CysSSCys = cystine
H_2S = hydrogen sulfide
Hb = hemoglobin
HOMO = highest occupied molecular orbital
K_{aff} = affinity constant
k_{int} = intrinsic rate constant
k_{off} = rate constant for ligand release
k_{on} = rate constant for ligand binding
MD = molecular dynamics
NO = nitric oxide
OEP = octaethylporphyrinate
Por = porphyrinate
QM/MM = quantum mechanics/molecular mechanics
TPP = 5,10,15,20-tetraphenyl porphyrinate
trHbO = truncated hemoglobin O of *Thermobifida fusca*